https://rbgeomorfologia.org.br/
ISSN 2236-5664

Revista Brasileira de Geomorfologia

v. 24, nº 3 (2023)

http://dx.doi.org/10.20502/rbg.v24i3.2425

Research Article

Paleoglaciological reconstruction and geomorphological mapping of Dobrowolski Glacier, King George Island, Antarctica

Reconstrução paleoglaciológica e mapeamento geomorfológico da geleira Dobrowolski, Ilha Rei George, Antártica

Cleiva Perondi[1], Kátia Kellem da Rosa[2] Fabio José Guedes Magrani[3] Carina Petsch[4] Rosemary Vieira[5] Arthur Ayres Neto[6] and Jefferson Cardia Simões[7]

[1] Programa de Pós-graduação em Geografia. Centro Polar e Climático, Instituto de Geociências da Universidade Federal do Rio Grande do Sul, Av. Bento Gonçalves, 9500, 91501-970, Porto Alegre - RS, Brasil. (51) 33087522. E-mail: cleiva.perondi@ufrgs.br
ORCID: 0000-0003-2202-2721

[2] Centro Polar e Climático, Instituto de Geociências da Universidade Federal do Rio Grande do Sul, Av. Bento Gonçalves, 9500, 91501-970, Porto Alegre - RS, Brasil. E-mail: katia.rosa@ufrgs.br
ORCID: 0000-0003-0977-9658.

[3] Universität Bern. Oeschger Centre for Climate Change Research & Institut für Geologie. Baltzerstrasse 1+3, 3012 Bern. Switzerland. E-mail:fabiomagrani@gmail.com
ORCID: 0000-0002-9487-5849

[4] Departamento de Geociências, Universidade Federal de Santa Maria (UFSM), Av. Roraima, 1000, Santa Maria, Rio Grande do Sul. CEP 97105-900. Brasil. E-mail: carina.petsch@ufsm.br
ORCID: 0000-0002-1079-0080.

[5] Instituto de Geociências. Departamento de Geografia da Universidade Federal Fluminense. Av. Gal. Milton Tavares de Souza, s/n 24210-346, Niterói/RJ. Brasil. E-mail: rosemaryvieira@id.uff .br
ORCID: 0000-0003-0312-2890.

[6] Departamento de Geologia e Geofísica da Universidade Federal Fluminense, Av. Gal. Milton Tavares de Souza, s/n 24210-346, Niterói/RJ. Brasil. E-mail: aayres@id.uff.br
ORCID: 0000-0002-2982-245X

[7] Centro Polar e Climático, Instituto de Geociências da Universidade Federal do Rio Grande do Sul, Av. Bento Gonçalves, 9500, 91501-970, Porto Alegre - RS, Brasil. Climate Change Institute, University of Maine, Orono, ME, USA. E-mail: jefferson.simoes@ufrgs.br
ORCID: 0000-0001-5555-3401

Received: 09/06/2023; Accepted: 09/08/2023; Published:19/09/2023

Abstract: The paper aims to reconstruct the fluctuations of Dobrowolski Glacier, a tidewater glacier located in the inner position of the Admiralty Bay (King George Island, Antarctica), from the Little Ice Age (1400-1700) until the present. Measurements of the glacier's area and length were based on multitemporal satellite imagery and submarine glacial landforms. The glacier surface area variations between the Little Ice Age and 2014 A.D were estimated. Morainic banks and paleoglacial reconstructions provided evidence of fluctuations in the surface area of the glacier between PIG and 2014 AD. Therefore, four stages of analysis were established: Stage I (Part I) (1400 to 1700), Stage I (Part II) (1700 until the mid-20th century), Stage II (mid-20th century until the 1980s), Stage III (1980 to 2000), and Stage IV (2000 to 2020). The climate during the Little Ice Age triggered the last major glacial advance, and their grounding line position was recorded by an external and prominent morainic

bank. After the major glacial advance position of the grounding line, the ice-margin has undergone higher retreat rates (stage I) as response to the warming trend and the loss of anchoring point. The stage II (Unit B) is recorded by distal and discontinuous morainal ridges and glacial lineations formed in the context of an active ice flow at a deeper point in the fjord. During stage III (Unit C) glacial lineations and steep slopes occur, while landforms are less preserved, revealing a fast shrinkage phase. Stage IV is characterized by discontinuous morainic ridges (Unit D), when the glacier presents the highest annual glacial area loss. Currently, the accelerated shrinkage may be linked to the loss of anchorage on seamounts (serving as pinning points) and increased warming. The U-shaped valley geometry has also influenced the glacier shrinkage processes and the redirection of glacial paleoflow during the last 300 years. The retreat rate to mid-20th century-2020 period is higher than Little Ice Age- mid-20th century period.

Keywords: Climate change; Glacial extent; Glacier reconstruction; Ice-margin; Little Ice Age; Morainal banks.

Resumo: O trabalho visa reconstituir a paleoglaciologia da Geleira Dobrowolski, uma geleira de descarga de maré na Baía do Almirantado (Ilha Rei George, Antártica Marítima), desde a Pequena Idade do Gelo (PIG) (1400-1700) ao presente. Foram utilizados modelos digitais de elevação, dados de batimetria, imagens de satélite multitemporais e interpretação de formas de relevo glaciomarinhas para as medições de área, comprimento e reconstruir o perfil superficial da geleira. Bancos morâinicos submarinos e reconstruções paleoglaciais mostraram as flutuações na área superficial da geleira entre a PIG e 2014 D.C. Portanto, foram estabelecidos 4 estágios de análise: I (parte I) (1400 a 1700) I (parte II) (1700 até meados do século XX) II (meados do século XX até a década de 1980) III (1980 a 2000) e IV (2000 a 2020). As forçantes climáticas durante a PIG desencadearam o último grande avanço da geleira até a posição da linha de aterramento em um banco morâinico externo e proeminente. Após a posição da linha de aterramento, em banco morâinico, durante a PIG, a geleira (estágio I) apresentou significativas taxas de retração com a perda de seu ponto de ancoragem em resposta à tendência de aquecimento. No estágio II, há ocorrência de bancos morâinicos distantes entre si, com cristas descontínuas e a presença de lineações glaciais formadas em um contexto de fluxo de gelo ativo quando a geleira Dobrowolski alcançava um ponto de maior profundidade do fiorde. Durante o estágio III ocorrem lineações glaciais e declive acentuado, embora feições de relevo sejam menos preservadas devido às altas taxas de retração. O estágio IV é caracterizado por cristas morâinicas descontínuas e a maior perda de área glacial anual. A geleira reduziu substancialmente sua superfície glacial depois de sair do ponto de ancoragem. A taxa de retração da geleira desde meados do século XX é maior do que a evidenciada entre o período correspondente a 1700 até meados do século XX.

Palavras-chave: Bancos morâinicos; Extensão glacial; Pequena Idade do Gelo; Mudanças climáticas.

1. Introduction

Glaciers' extent can be proxies for paleoclimate reconstruction at different time scales (decades to millennia), as they are present on almost all continents and sensitive to climate. Varying their extents as thicknesses during warm and cold periods, such as the Last Glacial Maximum (MACKINTOSH; ANDERSON; RAYMOND, 2016). Reconstructing glacial fluctuations contributes to the understanding of past, present, and future climate changes. Depositional features, such as moraines (ROSA et al., 2013, 2014b; MACKINTOSH; ANDERSON; RAYMOND, 2016; LIANG et al., 2018), can be a good record of glacial front changes.

Historical temperature series contribute to the understanding of glacial fluctuations. Mulvaney et al. (2012) carried out a study based on ice cores on James Ross Island and reconstructed the historical temperature series for the last 5,000 years BP. Evidence showed that ice shelves reached the vicinity of the northern sector of the Antarctic Peninsula during the Upper Holocene, by a cooling event starting from 2,500 years BP. In addition, the authors suggest a pronounced cooling stage as early as 600 BP. For the Antarctic Peninsula and the Southern Shetlands islands, recent environmental changes (20th and 21st century) were related to the global warming trend (SIEGERT et al., 2019; DZIEMBOWSKI; BIALIK, 2022). Temperature data for King George Island (KGI), presented by Kejna, Arazny, and Sobota (2013), show an increase of 1.2°C for the period 1948 to 2011.

Dating is another important element that supports the reconstruction of glacial environments. Paleoglaciological studies focus mainly on cycles of glaciations and deglaciations that occurred during the Quaternary, while methods for dating depositional events make it possible to extract the chronologies of glacial

events (FASTOOK; HUGHES, 2013). Geoforms are also widely used to support glacial information on different time scales (millennia, centuries, and decades; BENN & EVANS, 2010).

Geographic Information System has been used in several analyses and generation of models to interpret glacial extent (ROSA et al., 2014a; SIMÕES et al., 2015; ROSA et al., 2020; PERONDI et al., 2022; DZIEMBOWSKI; BIALIK, 2022). Thus, when using geomorphological proxies, it is important to have established at what scale we want to obtain information about the environment and which relief records are efficient for each scalar context.

This paper aims to reconstruct the paleoglaciology (area and length) of Dobrowolski Glacier since the Little Ice Age (1400-1700) through interpretations of the geomorphological record in the interscalar context and comparing with the glacial fluctuations evidenced since the mid-20th century through an ice core obtained from James Ross Island by Mulvaney et al. (2012).

2. Study Area

Currently, KGI has both marine terminus glaciers, such as Dobrowolski Glacier, and land terminus glaciers (PERONDI et al., 2020). The marine-glacial front glaciers are characterized by their cliff-like shape that allow the calving of icebergs (SIMÕES, 2004). Its frontal sector is in contact with the Martel Inlet (MI), located at the northern sector of the Admiralty Bay (Figures 1A and 1B). The Admiralty Bay is a Specially Managed Antarctic Area and an important area of interest for the Brazilian Antarctic Program, due to the presence of the Antarctic Station Comandante Ferraz – EACF in portuguese (Figure 1C).

Admiralty Bay's glaciers present steep gradients, with intense fracturing, and some present fast flow (ARIGONY-NETO, 2001). Different studies analyzed the retreat of glaciers in the area (ANGIEL; DĄBSKI, 2012; ROSA et al., 2020; PERONDI et al., 2022). As glaciers retreat, they expose depositional features which provide information about the glacial history of the site and ongoing changes.

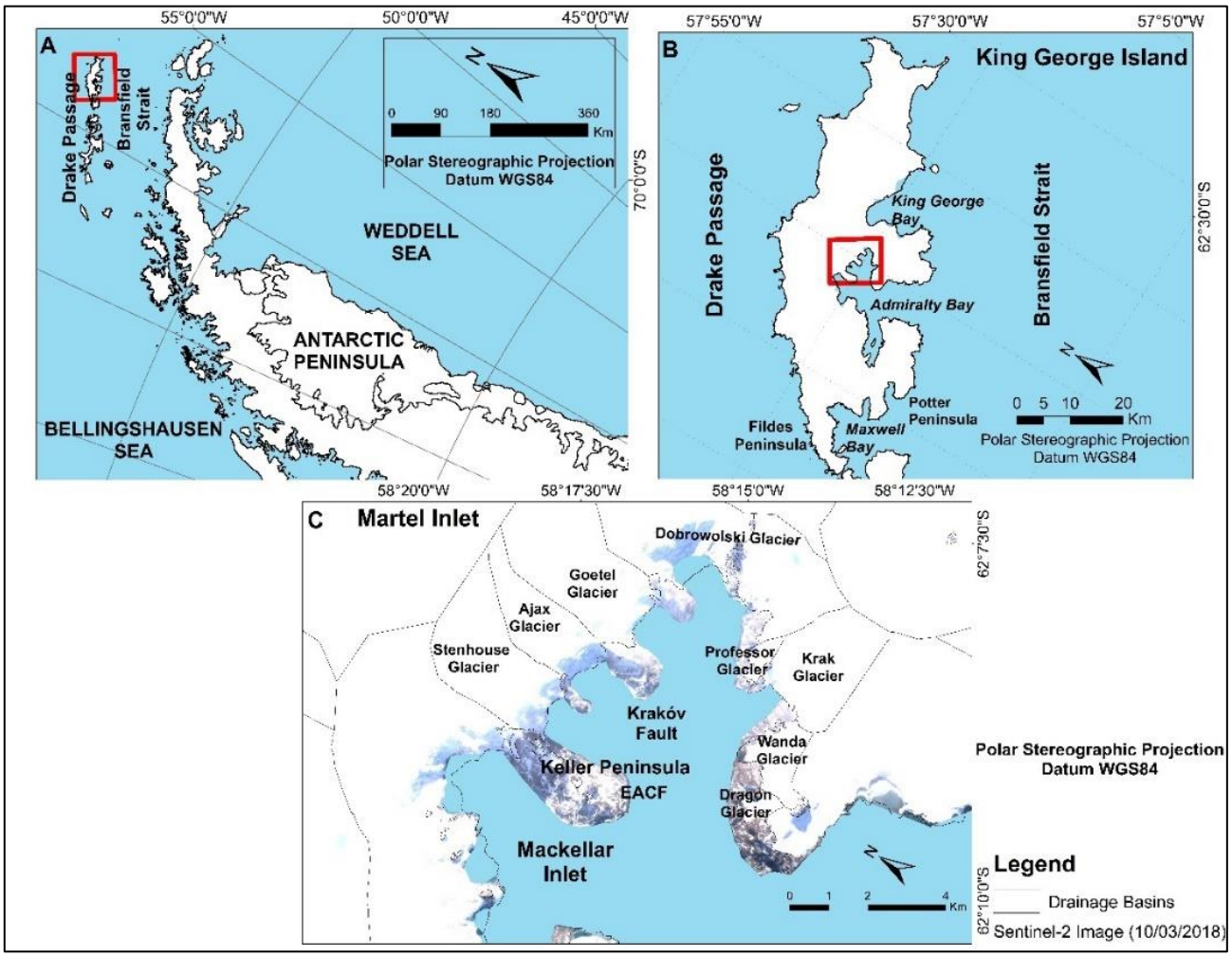

Figure 1. Location map. a) KGI location northeast of the Antarctic Peninsula. b) The inset red polygon is representing the location of Martel Inlet on KGI. c) Martel Inlet located along the Kraków Fault (with N-S orientation) and their current glaciers. Data source: Quantarctica (Matsuoka et al. 2018).

The climate in the South Shetlands region is classified as subpolar maritime (SETZER et al., 2004). During the summer months, the temperature may reach some degrees above 0 °C (RACHLEWICZ, 1997; BRAUN, 2001). The KGI is influenced by moisture from the Maritime Antarctic, with net precipitation occurring mainly during March and April (SETZER et al., 2004).

The island is associated with an extension of the Scotia Arc (CURL, 1980). This arc developed during the breakup of the Gondwana supercontinent, which led to the separation of southern South America from the Antarctic ridge (LIVERMORE; WOOLLETT, 1993), by a transcurrent fault zone (MALDONADO et al., 1998). Sedimentary, metasedimentary, volcanic, and intrusive igneous rocks from the Upper Jurassic, Upper Cretaceous to Miocene are observed in the island (BARTON, 1965). The Martel Inlet is connected to the Ezcurra fault system, which has NE-SW orientation, the Kraków fault, with N-S orientation, and both Barton Horst and Warszawa tectonic blocks (BIRKENMAJER, 1991).

Dobrowolski Glacier currently flows down valley. This valley has a topographic width of 355 meters, considering its drainage dividers and in its longitudinal profile has a topographic amplitude of 650 meters, considering the subaerial and submarine sectors.

3. Materials and Methods

This item aims at presenting the database and analysis techniques.

3.1 Interpretation of the length of Dobrowolski Glacier from the Little Ice Age

The measurements of Dobrowolski Glacier´s length and area were based on morainal records geomorphological (morainal banks), for the years of 1956, 1979, 1989, 1995, 2000, 2003, 2005, 2011, 2021 and satellite images or topographic charts. The data is composed of optical and SAR imagens (1979-2020), a Digital Elevation Model and multibeam bathymetry. The data was analyzed in ArcGIS™, QGIS, and CARIS softwares (Table 1).

Table 1. Orbital images and digital elevation model used in the present research.

Data/Sensor	Acquisition date	Band	Spatial Resolution	Type of Data	Source
SPOT/MSS	February 1989	3,2,1	20 m	Optical imaging	Polar and Climate Center of UFRGS
Landsat 4 TM	January 28, 1989	3,2,1	30 m	Optical imaging	https://earthexplorer.usgs.gov/
Sentinel-2B	January 19, 2020	2, 3, 4, 8 / 11	10 m and 20 m	Optical imaging	https://scihub.copernicus.eu/dhus/#/home
Sentinel-1 IW HH	March 20, 2020	C	5x20 m	SAR image	https://scihub.copernicus.eu/dhus/#/home
TanDEM-X	2016	X	12 m	Digital Elevation Model	https://doi.pangaea.de/10.1594/PANGAEA.863567
IBCSO	2013	-	500 m x 500 m	Digital Bathymetric Model	https://doi.pangaea.de/10.1594/PANGAEA.805736
Topobatimetric	2009/ 2017	-	4	Elevation and bathymetric model (multibeam)	Perondi et al. (2022)

In addition to the aforementioned data, shapefiles of the glacier front obtained in previous work by Rosa et al. (2013; for the years 2003, 2005, and 2011), Arigony-Neto (2001; for the years 1956, 1979, 1988, 1995, and 2000) and dating informations of the study area (YOON, 2000) were used. Shapefiles of drainage dividers were obtained from Global Land Ice Measurements from Space (GLIMS project). Bathymetric and shoreline information used to

delimit Dobrowolski Glacier derive from the Antarctic Digital Database (GERRISH et al., 2020) and Quantarctica (MATSUOKA et al., 2021) (Table 2).

Table 2. Vector databases

Shapefile	Year	Source
GLIMS	2000	https://www.glims.org/
Antarctic Digital Database	-	https://www.scar.org/resources/antarctic-digital-database/
Dados Quantarctica	-	https://www.npolar.no/quantarctica/
Shapefiles	1979, 1988, 1995, and 2000	Arigony-Neto (2001)
Shapefiles	2003, 2005, and 2011	Rosa et al. (2013)

For the atmospheric corrections on satellite images, a Semi-Automatic Classification add-on (CONGEDO, 2016) was employed, although the atmospheric correction was performed through dark object subtraction. The images were coregistered with a Sentinel-2B image (error < 1 pixel). An error in co-registration of ±1 pixel is permissible, as observed by other authors (NIE et al., 2013; LI et al., 2020). The RGB color compositions used were: 321 and 432 for the SPOT and Sentinel-2B scenes, respectively.

For the validation of the mappings, both Normalized Difference Snow Index and Normalized Difference Water Index were used, since these indices show an efficient method for the delimitation of glacial features (ALBERT, 2002). During the Brazilian Antarctic Operation (OPERANTAR) XXXVIII and XXXIX (2020 and 2021) photographs were taken showing the current environmental context of the studied site, such as ice-free areas and the ice-margin of Dobrowolski Glacier. The uncertainty of the length mappings was less than 0,06 km. The lowest uncertainty was 0,03 km for 2020 length measurements. The measurement error of the image mapping was based on the methodology of Li et al. (2015).

The identification of relief features was performed manually in ArcGIS, based on identification criteria proposed by Bennet & Glasser (1996), Ottesen & Dowdeswell (2006), Benn & Evans (2010), Streuff et al. (2015), and Wölfl et al. (2016). These criteria involve the morphology (discontinuous mounds or linear ridges, sinuous ridges), morphometrical characteristics, depositional environment, sedimentology, genesis (mass movement indicators, glaciotectonic deformation, and others), the context in the glacier (parallel or perpendicular to ice-flow). This approach applies sedimentological analysis and fieldwork photographs, high-resolution satellite images, digital elevation models, and geomorphometric data.

Geomorphometric data such as, slope, hypsometry, shading relief, and topographic profiles, supported by the interpretation of environments and landforms, through ArcGIS™ software. These products show depth values for each glacial stage, average slopes, the approximate number of depositional ridges across the ice, the average

distance between ridges across the ice, the scales of the ridges, and the fjord confluence factor. ArcGIS™ software was also used to map the morainal banks and the length of Dobrowolski Glacier.

The measurements of Dobrowolski Glacier´s length in Little Ice Age was inferred based on prominent outer morainal bank position (which demonstrate old extensions and grounding lines location). Morainal banks at this position in the fjord are similar with others observed by Wölfl et al. (2016) at Potter Cove, KGI, and also related to the Little Ice Age.

3.2 Interpretation of the evolutionary stages of Dobrowolski Glacier

The evolutionary stages of Dobrowolski Glacier were interpreted based on the characteristics of the relief features of the study area, such as the morainal banks and the bathymetric data as performed by Oliva et al. (2019) and Petsch et al. (2020). Four stages were established: Stage I (Part I) (1400 to 1700), Stage I (Part II) (1700 until the mid-20th century), Stage II (mid-20th century to the 1980s), Stage III (1980 to 2000), and Stage IV (2000 to 2020). The parameters observed for the delineation of the stages comprise the distance from the present glacial front line, depth, and structures of the relief features. The retreat rate was estimated for each period.

3.3 Variation of the glacier surface of Dobrowolski Glacier since the Little Ice Age

The downstream-upstream glacial surface variation from the Little Ice Age was obtained using a similar approach as performed by Benn & Hulton (2010). The approach uses bedrock values and known target elevations to calculate the glacial surface. To reconstruct the 2D topographic profile, the subglacial bedrock values provided by Bedmap2 (POPE, 2017) and the digital bathymetric model (current subsea sector) were considered. To obtain the distance values between the end of the glacier and visualize the elevation values of the bedrock embayment, topographic profiles were drawn using ArcGIS™.

For the year of 2014, the elevation values provided by TanDEM-X (2014) were used to generate the glacial surface of Dobrowolski Glacier. Its glacial surface since the Little Ice Age was inferred based on nunataks and trimlines that contained the glacial cover of 1988 (Figure 2). It is thus assumed that the highest point of these features would also be under the ice (but not very thick) during the Little Ice Age.

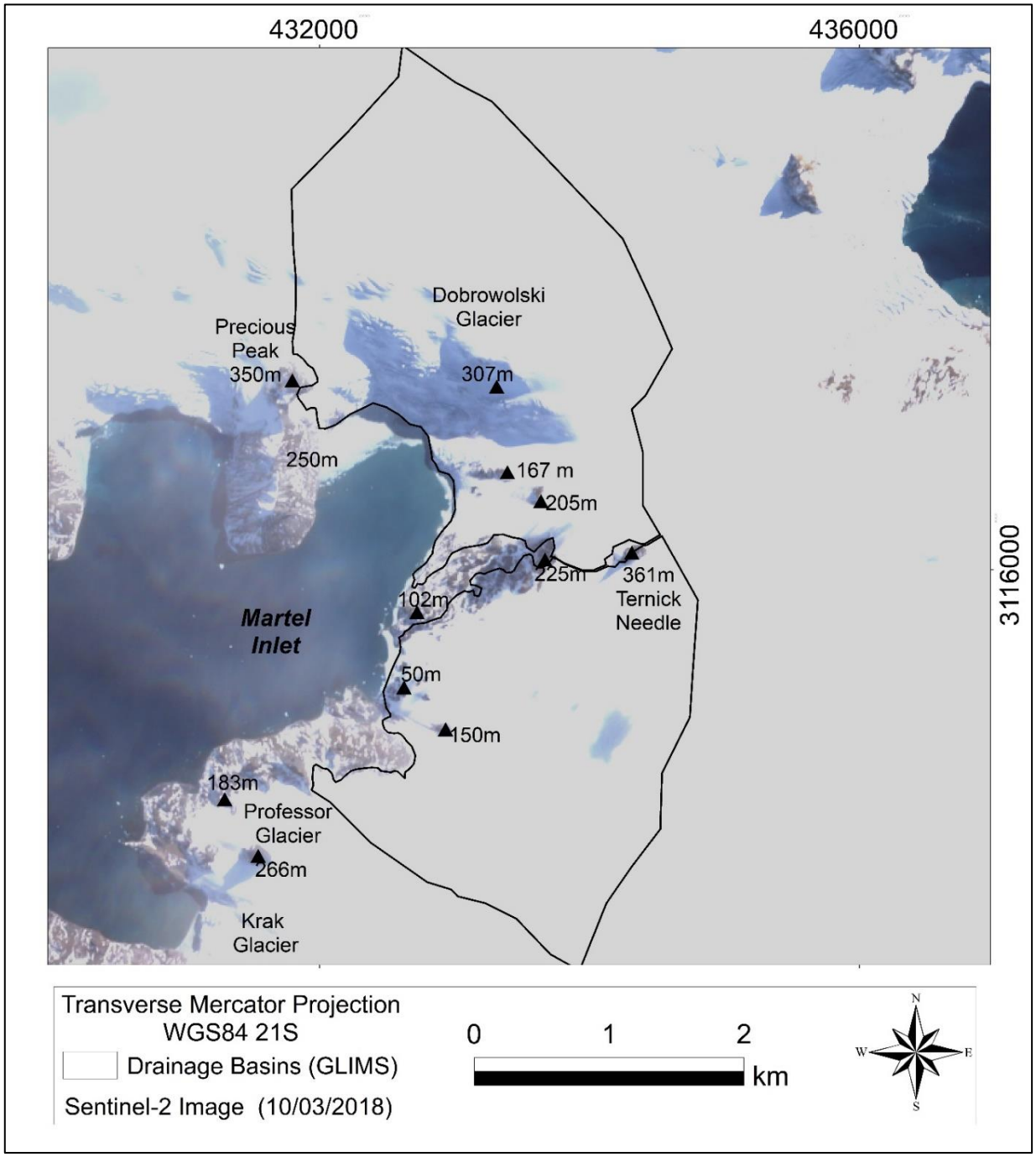

Figure 2. Rock outcrops and highest topographic points in the study area.

To calibrate the model, the target elevation peaks (Fig. 2) were obtained based on observing landforms on satellite images with true color band composition and obtaining elevation values (using TanDEM-X Digital Elevation Model) of points covered by ice for each analyzed period. The source of the satellite images were: SPOT (1988, 1995, and 2000), Sentinel-2 image (2018), and PlanetScope image (2019).

4. Results

4.1 Length fluctuations

The Dobrowolski Glacier showed fluctuations in its length since the Little Ice Age recorded through morainal banks and satellite images. It had an estimated total length of 4.3 km during the Little Ice Age. During the last decades, the glacier extension retreated from 3.8 km, in the middle of the 20th century (1956-1979), to 3.5 km, in 1988/89, to 3.1 km, in 1995, and 2.8 km, in 2000. Currently (2020 and 2021), the total length is 2.3 km (Table 1), which represents an overall decrease of ~46% in length (LIA until 2021).

Table 3. Area (km²) and length (km) data of Dobrowolski Glacier variation.

Period	Little Ice Age	Mid-20th century	1988/89	1995	2000	2020/21
Length (km)	4.3	3.8	3.5	3.1	2.8	2.3
Area (km²)	9.2	8.2	8.1	7.5	7.3	6.7

4.2 Area and glacier surface

Dobrowolski glacier showed a decrease in extent and area. In recent decades, the area varied from 8.2 km², in 1979, to 8.1 km², in 1988/89, from 7.5 km², in 1995, to 7.3 km², in 2000, and, recently, in 2021, the area of the glacier was 6.7 km² (Figure 3A and Table 3).

Dobrowolski Glacier showed fluctuations in its glacial surface (glacier thickness and elevation) between Little Ice Age and 2014. The profile (Figure 3B) represented the frontal margin of Dobrowolski Glacier and the surface variation between the Little Ice Age and the 21th century (2014/2020). During the Little Ice Age (Figure 3B, purple line), the glacial surface of Dobrowolski Glacier reached approximately 4,400 m in length and a prominent outer moraine in its frontal position. The glacier presented a maximum elevation of 550 m, 250 m thick in the accumulation area, and 90 m at its grounding line. In the current decade (2020), the glacier was 2,200 m long, with a maximum elevation of 525 m and 225 m thick. The present glacier front has a marine terminus, in which it is possible to observe a basement outcrop. The front was estimated to be 4 m above sea level (Figure 3B).

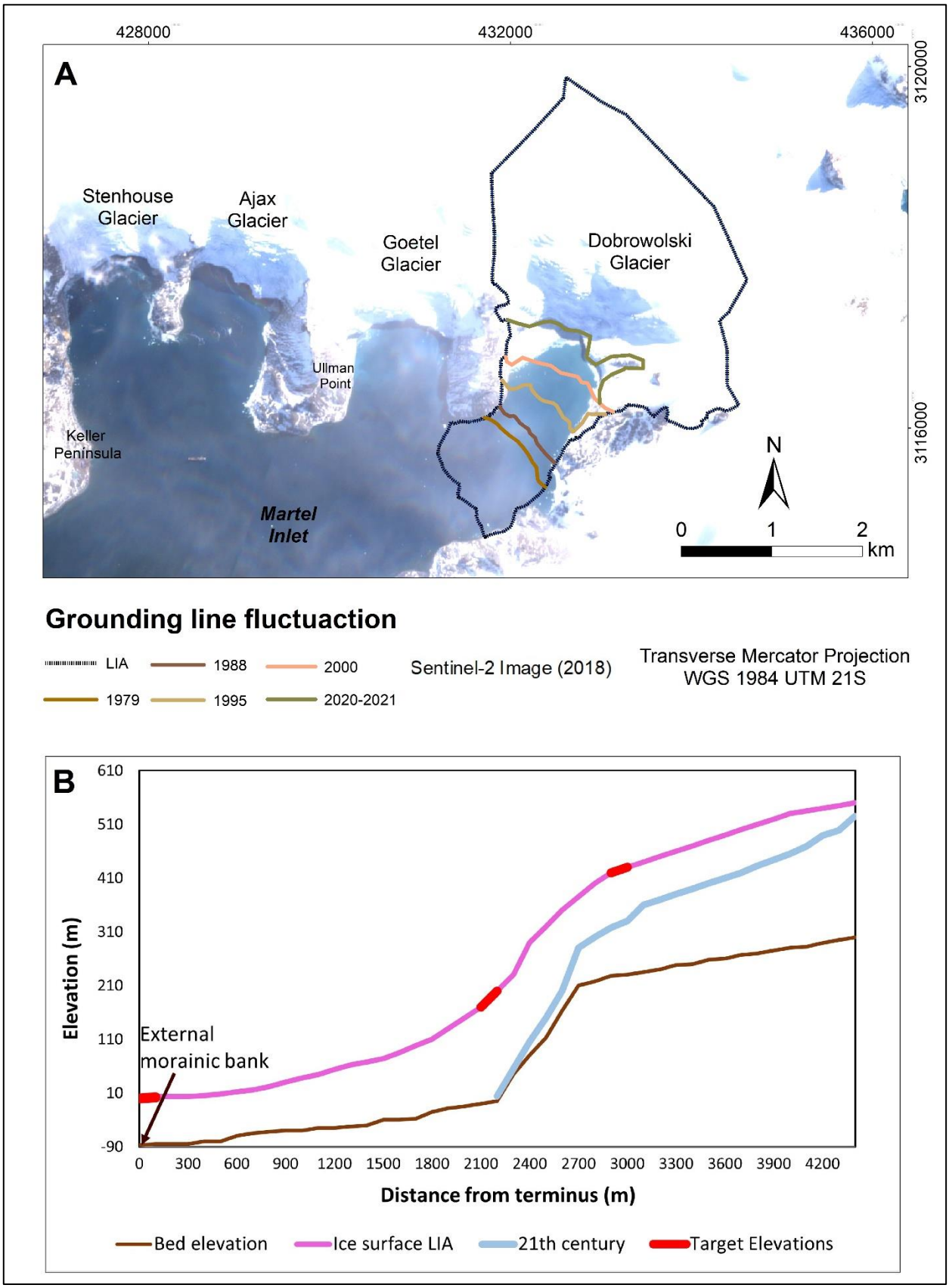

Figure 3. A) Grounding line fluctuations of the Dobrowolski Glacier. B) Topographic profile of the Dobrowolski Glacier between the Little Ice Age and the 21th century (2014/2020). Target elevations are based on nunatak and trimlines features, as illustrated in figure 4A.

4.3 Retreat rate pattern

Between 2000 - 2005 the shrinkage was approximately 50 m/yr. For the period 2005 - 2011, the shrinkage rate was ~79 m/yr. Between 2011 and 2021, the shrinkage rate remained high (around 14.5 m/yr).

4.4 Geomorphological units of Dobrowolski Glacier and its stages

In the glacial drainage basin of Dobrowolski Glacier, nunataks and aretes are observed in the subaerial sector. In the submarine environment morainal banks are identified (Figure 4). The morainal banks belong to units I to IV, as shown by the bathymetric data and their geomorphological characteristics (Figure 4A).

The geomorphological units indicate the evolutionary stages of the grounding line since the Little Ice Age (Figure 4B). Stage I is the most distant from the present glacial margin and the oldest, formed in the last hundreds of years (until the mid-20th century). It is subdivided into two parts:

a) Stage I - part I - between 1400 and 1700 during a neoglacial event known as the Little Ice Age; Part I has a higher number (35) of continuous ridges when compared to the other stages (between 19 and 7) and in shallow depths and slopes (except for the distal sectors of each morainal bank).

b) Stage I - part II - after 1700. The ridges of this unit are prominent and recognized as macroscale forms (greater than 30 meters in elevation and width) and mesoscale forms (less than 20 m). Part II is distinguished for presenting fewer ridges, greater distances between them, being in a sector of greater depths and presenting glacial lineations.

Stage I is interpreted by landforms in the distal sector of the present front of Dobrowolski Glacier (approximately 2,200 m), where there is a prominent outer morainal bank (MB1; Figure 4A and Figure 5B and 6B). MB1 is interpreted as the position of maximum glacial extent in the Little Ice Age (Figure 6B). Another extensive morainal bank was also identified in the southeastern part of the inlet and may records the position of a last stabilization during the Little Ice Age (MB2; Figure 4A). Other, less prominent, sometimes discontinuous, morainal banks occur in the inner sector of the inlet (Figure 4A). Glacial lineations occur in the submarine environment close to the actual glacier front.

Stage II, formed in the mid-20th century until the end of the 1980s (1988/89), presents has the crests of the morainal banks with crests which are more spaced distant (20 to 40 m) from each other and sparse. These morainal banks lose continuity and are identified as glacial lineations.

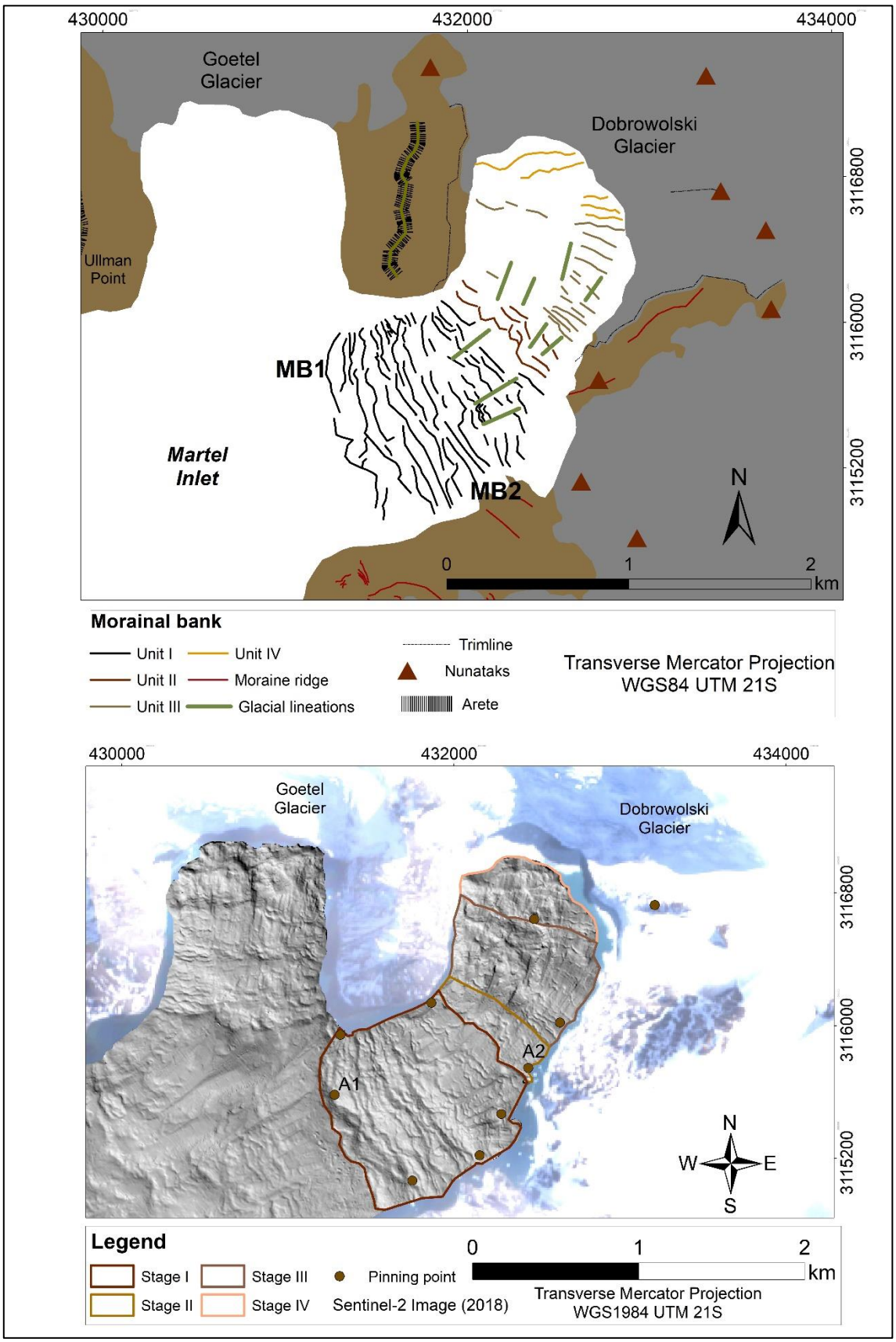

Figure 4. Geomorphological evolution of Dobrowolski Glacier. A) Morainal banks identified in the submarine sector near the current front of the Dobrowolski glacier. B) Geomorphological units and stages of Dobrowolski Glacier.

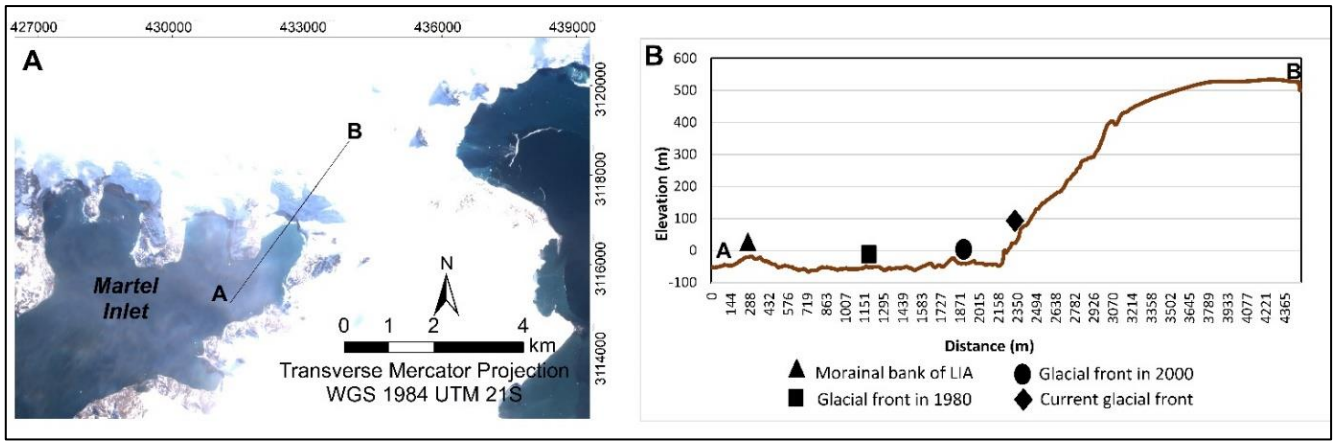

Figure 5. A) Topographic profile over location map of Martel inlet and Dobrowolski glacier. B) Submarine and subaerial topographic profile. Letter A indicates the beginning of the profile and B the end of the profile.

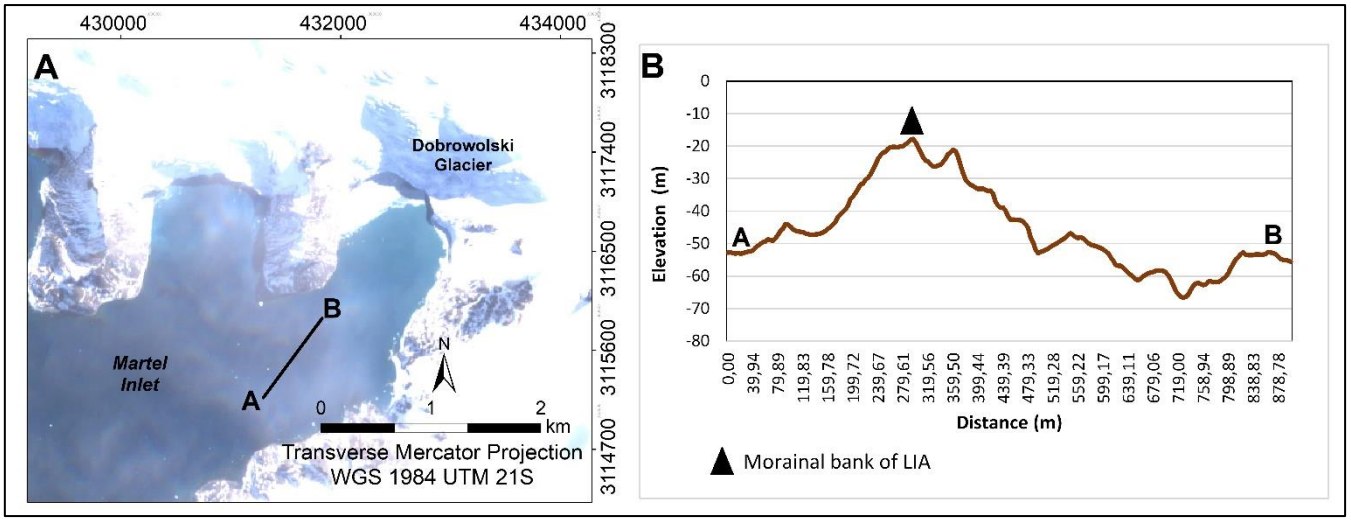

Figure 6. A) Topographic profile location map in Martel inlet. B) Glacial pinning point recorded by morainic bank of Little Ice Age. Letter A indicates the beginning of the profile and B the end of the profile.

Stage III, formed in the late 20th century (between 1988/89 and 2000), has fewer preserved morainal features (19) compared to Stage I; glacial lineations were identified on steep slopes.

The most recent stage, IV (last two decades), shows a reduction in morainic banks (5) and greater spacing (20 to 90 m) between them (Table 4). The proglacial area is characterized by steep slopes and the absence of glacial lineations. Currently, the front of Dobrowolski Glacier is 694 m wide and flows through a constrained valley.

Table 4. Stages of Dobrowolski Glacier fluctuations.

Geomorphological unit	I	II	III	IV
Stage of the evolution of the grounding line	I	II	III	IV
Bathymetry (m)	**Part I:** Minimum: -70	Min: -99 Average:	Min: -92.7 Average:	Min: -69 Average:

	Average: -32.5 **Part II:** Minimum: -90 Average: -50	-58	-47.5	-40
Average slope (°)	14	15	17.5	17
The approximate number of depositional ice transverse ridges	Part I: 35 Part II: 39	11	19	5
Average distance between ice transverse ridges (m)	15 (for the macroforms in part I) to 20 (for the mesoforms in part II)	20 to 40	15 to 80	20 to 90
Scale (dimensions of the ice transverse ridges)	Macro to mesoforms	Mesoforms	Mesoforms	Mesoforms
Fjord confluence factor (average width in m)	1,398 (part I) 1,016 (part II)	748	840	789
Glacial shrinkage rate (m/year)	2 (part I) e 1.8 (part II)	5.5	46	27.66

5. Discussion

In general, the geomorphological features used as indicators of glacial morphological evolution can be found in both submarine (Admiralty Bay Fjord) and subaerial (ice-free areas on KGI) environments and demonstrate distinct processes occurring at different time scales. Glacial relief features showed information at different scales (from decades to hundreds of years), as well as, cartographically, being observed at different scales. Dobrowolski Glacier fluctuations responds to climate variability of hundreds of years, such as the Little Ice Age and other Holocene fluctuations, which are well noticed at a scale of 1:100000v; whereas glacial fluctuations, related to the increase in average atmospheric temperature in recent decades, are visualized at a scale of 1:5000.

Glacial geomorphological proxies have been important for paleoglaciological reconstruction. They are preserved for long periods and can be identified in the landscape by on-site reconnaissance, high-resolution satellite images, and multibeam bathymetric data. Their resolutions should be used according to the scale of the feature one wishes to analyze. Geospatial data, such as geomorphological mapping, Digital Elevation Models, and GIS, were used for the reconstruction of paleo-glacial extent. The integration between the data was fundamental to the reliability of the result.

5.1 Stage I

Stage I is the oldest, with a prominent outer morainal bank with elevations ranging from 30 to 60 meters, a length of 675 meters and a width of 50 meters. Unit I (Figure 4) represents the stage I and presents some similarities to features found in the proglacial sector of the Collins Glacier, also called Bellingshausen Dome (Fildes Peninsula, KGI) (HALL, 2007). This morainal bank has been related to a Neoglacial period that occurred approximately 600 years ago, representing climate variability on a long-time scale, as pointed out by several authors such as Mulvaney et al. (2012) and Abram et al. (2013).

In the period between 1400 and 1700, approximately, temperature showed a decreasing trend on a long-term scale (Neoglacial Period) and a decrease in melting that may be linked to the pronounced cooling of the Little Ice Age (Hall (2007).

According to data reconstructing air temperature anomalies from about 1400 onwards (MULVANEY et al. 2012), there was a significant decrease in atmospheric temperature (also accompanied by a decrease in glacial melt). At this stage, marked by further advance, the position of the grounding line has stabilized in the fjord at various positions, due to topographic anchoring points (pinning points; 4B). This has led to stage I of glacial evolution when considering the time since the Little Ice Age. For marine environments, Dowdeswell et al. (2008) state that larger morainal banks record long stages of grounding line stabilization, likely lasting for centuries.

After 1800, an increase in temperature was observed, also accompanied by peaks of glacial melt. For Dobrowolski Glacier, the series of submarine morainal banks reveal how the glacier retreated after the Little Ice Age and how fast this process happened after the second half of the 20th century.

There are interspersed morainal banks and small-scale lineations in the space of stage I (part II), which show evidence of a wet basal thermal regime, since for its formation they require abundant water at the ice/rock interface, as stated by Powell and Alley (2013).

5.2 Stages II and III

During stage II, Dobrowolski Glacier found some anchor points, such as rocky areas (Figures 5 and 6). The presence of shallow sills and narrow sections of the fjord were identified in expressive morainal bank location (Figure 6). The stage II stabilization is recorded by these morainal banks. These pinning points in local fjords helped to control the stability of ice fronts and glaciers, maintaining stable terminus positions for many decades while other adjacent non-anchored glaciers underwent retreat (BENN et al., 2017; BIANCHI et al., 2020).

Both stages II and III came after Dobrowolski Glacier lot its anchorage of stage I. In this period (1980s to 2000s, approximately), the widely spaced morainal banks showed less significant ridges compared to the previous stage I. The glacial fluctuations, loss in surface area (2.4 km²) and length (2 km) can be related to the climatic fluctuations that occurred in the last three centuries until the end of the 20th century (Figures 5 and 6). The detachment from a pinning point in stage I initiated episodes of rapid thinning and retreat of the glacier, which caused the differences observed in the distance between the morainal banks.

The narrow sections of the fjord became higher in later stages (II), and the presence of an active glacial flow passing through sectors of stages II and III may explain the formation of mesoscale glacial lineations in that period. Glacial lineations are indicative of the direction of active fast-flowing glaciers (DOWDESWELL et al. 2004) and suggest a wet thermal-based glacier (BENN & EVANS, 2010).

The water depth at the grounding line was deeper at stages II and III than at the current stage and stage I, implying a high retreat rate in stages II and III. The fjord depth can influence ice-calving processes and loss of glacial mass in this period. Studies by Hill et al. (2018) and Thomas et al. (2018) state that glaciers anchored at deeper marine depths exhibit high levels of shrinkage when compared to those anchored in shallower areas, as at

greater depths the glacier can experience greater basal and lateral friction, influencing ice-calving processes. Other authors, such as Braun & Goßmann (2002), also ratify greater losses for glaciers anchored at greater depths in the fjords.

During stage III there are records of glacial advance in the mid-1950s for some glaciers flowing into Martel Inlet, such as the Stenhouse Glacier. During 1957/1958, its glacial front underwent a great oscillation during the summer, with a significant detachment causing its front to retreat.

However, over the winter, the glacier advanced 150 m, followed again by a retreat in the following summer months (BRAUN et al., 2001). Thus, it is possible that the Stenhouse glacier has advanced together with adjacent glaciers. Another possibility is that the fronts mapped for the years of 1956 to 1970 may have been floating, since they do not coincide with the geomorphological record of moraines.

5.3 Stage IV

Stage IV shows the evolution of the modern sedimentary environment proximal to the Dobrowolski glacier front. Mulvaney et al. (2012) and Abram et al. (2013) show high rates of shrinkage as in stages III and IV, through an increased glacial melt. According to Kejna, Arazny, and Sobota (2013), the last five decades are related to an increase of the atmospheric warming at KGI and the consequent melting of glaciers.

The fast rates of grounding line retreat in stage IV also are linked to the increase in slope for the entire sector. According to Huybrechts & De Wolde (1999) and Schäfer et al. (2015), the loss in thickness with a grounded margin on the seabed is conditioned mainly by the climate. However, the steepening of slopes in the frontal sector leads to increased ice flow in the ablation zone, which, in turn, accelerates glacial mass loss. For the Antarctic Peninsula, Simões (2017) also suggests that the slope is an important glacial response to atmospheric temperatures, which has been increasing in the last decades. The formation of relief features transverse to the ice flow direction in the grounding line zone, between 1995 and 2000, as mesoscale morainal bank is well preserved, especially in the lower slope sector of the seafloor profile. The smaller and more closely spaced annual morainic features evidence high rates of glacial ablation and retreat (as also observed by BRADWELL; SIGURÐSSON; EVEREST, 2013).

The larger features, on the other hand, identified as glacial lineations, formed before the morainal banks, probably when the glacier was thicker and flowed towards the middle of the fjord, as indicated by Perondi et al. (2022). Glacial relief features, such as submarine morainal banks, recorded the history of the Dobrowolski Glacier. Aretes, lineations, and morainal banks were used as geomorphological proxies according to the temporal scale of analysis and the context they represent. Mapping and interpreting the paleoglaciology of complex areas were facilitated by combining remote sensing data and integrating them into a GIS, as also stated by Evans et al. (2014) and Chandler et al. (2018).

5.4 Climate input and variations in glacial extent

During the neoglacial event, the frontal section of Dobrowolski Glacier reached approximately 2.1 km from its present front (Figure 5). At this stage, the glacier front was anchored, forming a more prominent bank relative to the more recent ones. This advance was conditioned by significant temperature drops that occurred between 1400 and 1700. The Dobrowolski Glacier variation is a response to the oscillations in air temperature that have occurred over the last few centuries and the last few decades.

Distal to the current glacial front, there is a prominent moraine that indicates a long stabilization period of the glacial margin, reminiscent of the Little Ice Age. This kind of geomorphological proxy may be preserved for long periods, documenting features related to glacial length, thickness, and flow direction (BENN; EVANS, 2010). Other authors, such as Trueba & Cañadas (2004), also measured area variations in glaciers in the Cantabrian Mountains

in northern Spain using depositional and erosional forms since the Little Ice Age. The recent area and length changes of Dobrowolski Glacier are linked to the temperature oscillations that have occurred in recent centuries. It was observed that the glacial retreat in the study area in the last decades has been the most intense since the Little Ice Age. This acceleration in glacial retreat may be occurring due to the increasing temperature trends recorded for the Antarctic Peninsula region over the last five decades of the 20th century (RÜCKAMP et al., 2011; KEJNA; ARAZNY; SOBOTA, 2013; PERONDI et al., 2020; LORENZ, 2021).

5.5 Variations in the glacier surface since the Little Ice Age

At the time of the Little Ice Age, the Dobrowolski Glacier had a greater length and thickness compared to 2014. During the Little Ice Age, the glacier was at an elevation of 170 m and a thickness of 145 m in its actual frontal portion. In 2014, its thickness decreased to 30 m.

The paleoglacial reconstruction model, according to Benn & Hulton (2010), is a consistent tool for ancient glacier profiling. For the case of Dobrowolski Glacier, it enabled the understanding of the variation in thickness and elevation over time. Combined with other existing environmental information, a significant fluctuation in its configuration is observed, such as changes in its surface morphology – thickness of its frontal area, from the Little Ice Age to the present day.

Dobrowolski Glacier showed, through morainal banks on the seabed and the paleoglacial reconstruction profile, a continuous retreat since the Little Ice Age. This process responds to climatic variables and is linked to factors that lead to changes in glacial behavior (flow velocity and glacial mass loss). However, other non-climatic factors also exert control over this progression, such as internal glacier dynamics, topography, and bedrock lithology (GLASSER et al., 2005).

The glacier front was positioned in shallower marine conditions during the Little Ice Age (30-meter depth, approximately), but, in the 20th century, was at greater depths (80 to 90 meters, approximately; stages II and III). Deeper waters lead to greater mass losses, through tidally-influenced ice-calving rate and melting, linked to water temperature. The anchoring of the glacier in deep marine sectors shows higher levels of shrinkage compared to those that have their front in shallower sectors (THOMAS et al. 2018). Thus, with the end of the Little Ice Age cooling, the glacier may have reflected diminishing sea ice and deeper marine conditions. Melting led to a reduction in ice thickness combined with an accelerated ice–calving at the ice front, leading to further retreat (SIEGERT et al., 2022).

In the last two decades (stage IV) it is observed that the glacial retreat of Dobrowolski Glacier decreased (Table 3), which can be explained by the shallower depth of the anchorage point of its front (approximately 20 m) and the cooling trend of air temperature in the early 2000s. Whereas in the previous stages II and III, besides the glacier being anchored in deep marine sectors, it also coincides with peaks of temperature increase and glacial melt.

Authors such as Turner et al. (2016) and Oliva et al. (2017) have recorded in their studies a cooling trend in air temperature for the Antarctic Peninsula region between the late 1990s and 2014, compared to an increase in atmospheric temperature observed in the previous decades (OLIVA et al., 2017).

In the proximal environment of Dobrowolski Glacier, nunataks (Figure 7), indicate paleo glacial thickness, as they reveal the uplift of the bedrock. The nunataks exposed today are a good indicator of ancient glacial thickness, as denoted by Ballantyne (2007).

In the last 50 years, large areas of KGI have become ice-free and new nunataks (Figure 7) have appeared, which can be observed on satellite images, demonstrating a reduction in glacial thickness simultaneously to the process of glacial retreat (PUDEŁKO et al., 2018). The studies by Osmanoğlu et al. (2013) demonstrate that the

glaciers of KGI show retreat and lowering of the surface in recent decades, concomitantly with an increase in atmospheric temperature.

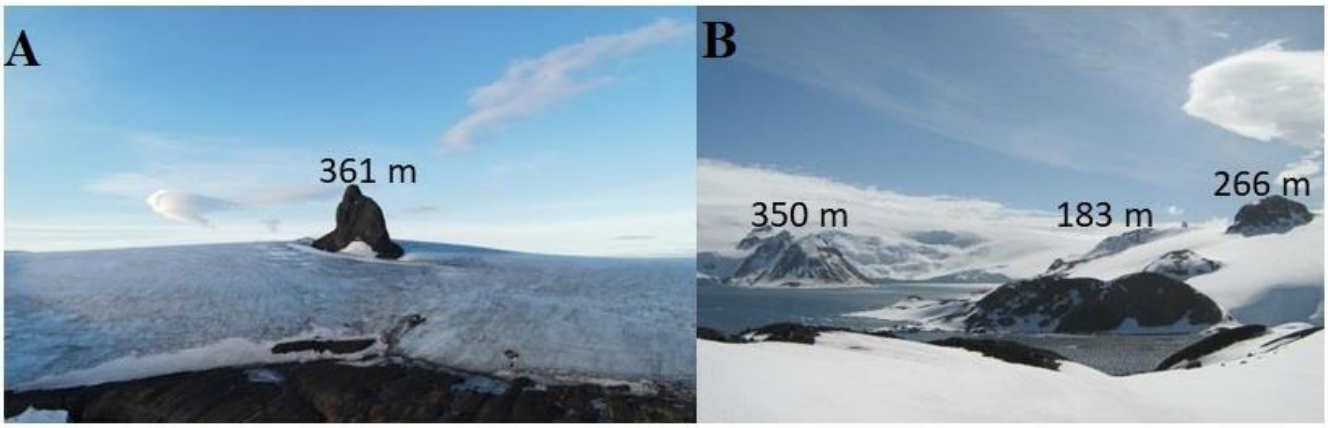

Figure 7. Nunataks present in the study area. A) Photography obtained by Santos Nascimento, 2020. Figure B) Photography obtained by Vieira, 2010.

In Dobrowolski Glacier's adjacent areas, trimlines can be also observed in satellite images and field photographs. These periglacial features record the position of the past glacial margin and thickness at different times. The trimlines are represented by erosional features on rock outcrops, which were covered in 1988 and assumed to have been so during the Little Ice Age. These relief features date back to the Little Ice Age period when they were covered by the glacier (Figure 4A).

The outer morainal bank is more prominent concerning the others and located closer to the edge of the present glacier. It is a feature with different heights along its crest, which may occur due to the reworking of sediments by marine action, and mass movements, among others, and because these points correspond to places where the glacier was anchored for a longer period during the Little Ice Age. Dowdeswell et al. (2008) argue that larger moraines indicate longer grounding line stabilization time. According to Abram et al. (2013), the decrease in the glacial melt during the Little Ice Age may be linked to the significant temperature decrease that occurred between approximately 1400 and 1700.

Towards the present front of the glacier, in the submarine environment, smaller morainal banks are observed, demonstrating shorter anchoring times of the glacier succeeded by retreat. These banks were formed in more recent periods (20th and 21st centuries), coinciding with the atmospheric warming trend recorded after the Little Ice Age, as pointed out by Mulvaney et al. (2012) and Abram et al. (2013).

Currently, the accelerated ice loss presented by the Dobrowolski Glacier may be linked to its anchorage loss. Rosa et al. (2014b) state that, because of its location in an area of steep rocky bedrock, it flows with more velocity and, when in contact with the sea, there is a calving of growlers. Thus, there is an increase in area loss, due to the lack of anchorage on the rocky-seamounts and submarine morainal banks.

5.6 The control of bedrock topography and fjord geometry

During the Little Ice Age, the Dobrowolski Glacier had its front section anchored on a topographic ridge (pinning point). Later, a rapid glacial retreat may also have occurred due to the loss of anchoring. Topographic highs in the submarine environment (Figure 5 and 6) can serve as pinning points for glaciers (Figure 4A), which gives them greater frontal stability. With the loss in thickness, the glacier may shift from this anchor point, leading

to further enhanced shrinkage (SMITH et al., 2017; BIANCHI et al., 2020). This condition could be explain the spaced morainal banks units (after II stage).

The steep slope of the frontal part of Dobrowolski Glacier, related to the basement topography, lithology, and a high structural control, causes ice to flow faster and reduces ice accumulation at small glacial drainage basins, favoring its mass loss.

The Martel Inlet fjord, where the Dobrowolski Glacier flows into, has well-known tectonic faults (BAS, 1969), such as the Ezcurra and Kraków faults, with NE-SW and N-S directions, respectively (BIRKENMAJER, 1991). These faults condition the arrangement and direction of glacial flow, which may also have influenced the change in flow direction since the Little Ice Age, via bedrock geometry (FITZPATRICK et al., 2013).

In glaciomarine environments, the fluctuations of the frontal position of a tidewater glacier are strongly controlled by its velocity, ice-calving rate, basal unstable areas, bedrock topography, and climate. Thus, bathymetry and topography together exert an important control on the response of tidewater glaciers to climate change (BIANCHI et al., 2020).

Other factors may also condition glacial retreats, such as the decrease in sea ice and precipitation control. Studies have shown that the recent increase in atmospheric temperature is linked to the reduction of sea ice and increment of sea temperature, generating greater basal melting for discharge glaciers (RIGNOT; STEFFEN, 2008), which is not the scoop of the present work but remain as a possible focus for future studies.

6. Conclusions

A chronology of glacial depositional landforms was proposed. We obtained the signal of changes since the Last Interglacial through the interpretation of landforms in the study area. Dobrowolski Glacier presents four stages of grounding line evolution, as a response to climate variability on long- and recent-time scales. Geomorphological data provide records of the evolution of ice-margin fluctuations and advances, such as the several preserved landforms, especially those exposed for less time, as post-1970s. The ice-marginal depositional forms in this environment were formed in recent decades and susceptible to rapid reworking. In areas exposed for longer (Stage I), the glacier influence becomes less evident in the ice-marginal sector and the depositional forms are less preserved.

With the evolution of retreat of Dobrowolski Glacier, there are records of grounding line stabilization (in stage I), inferred from the presence of a more external and prominent morainal bank (as well as other morainal banks, in Unit I, part I). The aforementioned morainal banks and stage were identified as from the Little Ice Age, when the grounding line advanced mainly due to a decrease in temperature. Part II of Unit I, on the other hand, represents long periods of glacial retreat and a few periods of glacial front stabilization.

Dobrowolski Glacier showed accelerated retreat after the detachment from a pinning point in stage I. The stage II initiated episodes of rapid thinning and retreat of the glacier. The frontal retreat process is recorded by morainal banks that are preserved in the submarine environment as paleo-front positions. Stages III and IV (between late 20th century and early 21th century) record morainal banks and rocky mounts that served as grounding points for the glacier in its margin. Both stages are more recent and near the frontal margin of the glacier.

Although the scarcity of studies regarding landscape evolution and reconstructions of recent changes in glacier extent (20th and 21st century and older, including Little Ice Age – 250-450 years AP), especially in Antarctica, the present work shows the possibility of identifying that the rate of glacier retreat observed in the last six decades is greater than that evidenced in the centuries preceding the 20th century. The glacier has substantially

reduced its glacial surface after exiting the condition influenced by a pinning point. We assessed different factors to delineate the glacier changes.

The results of this study also demonstrate the need for an inter-scale context when analyzing landscape evolution over time.

Author's contributions: All authors analyzed the data and wrote the paper.

Acknowledgements: We acknowledge the Conselho Nacional de Desenvolvimento Científico e Tecnológico (CNPq) Project 465680/2014-3 (INCT da Criosfera), Coordenação de Aperfeiçoamento de Pessoal de Nível Superior (CAPES), Brazilian Antarctic Program (PROANTAR), Foundation of Research Support of the State of Rio Grande do Sul (FAPERGS) for financial support, and Postgraduate Program in Geography of the UFRGS.

References

2. ABRAM, N.J.; MULVANEY, R.; WOLFF, E.W.; TRIEST, J.; KIPFSTUHL, S.; TRUSEL, L.D.; VIMEUX, F.; FLEET, L.; ARROWSMITH, C. Acceleration of snow melt in an Antarctic Peninsula ice core during the twentieth century. **Nature Geoscience**, v. 6, n. 5, p. 404-411, 2013. DOI: 10.1038/ngeo1787
3. ALBERT, T.H. Evaluation of Remote Sensing Techniques for Ice-Area Classification Applied to the Tropical Quelccaya Ice Cap, Peru. **Polar Geography**, v. 26, n. 3, p. 210–226, 2002. DOI: 10.1080/789610193
4. ANGIEL, P. J.; DĄBSKI, M. Lichenometric ages of the little ice age moraines on King George Island and of the last volcanic activity on Penguin Island (West Antarctica). Geografiska Annaler: Series A, Physical Geography, v. 94, n. 3, p. 395–412, 2012. DOI: 10.1111/j.1468-0459.2012.00460.x
5. ARIGONY-NETO, J. **Determinação e interpretação de características glaciológicas e geográficas com sistemas de informações geográficas na Área Antártica Especialmente Gerenciada Baía do Almirantado, ilha Rei George, Antártica**. Dissertação (Mestrado em Sensoriamento Remoto). Universidade Federal do Rio Grande do Sul. Porto Alegre-RS. 2001. 98 p.
6. BALLANTYNE, C.K. Glacial landforms, ice sheets: Trimlines and palaeonunataks. **Encyclopedia of Quaternary Science**, p. 892-903, 2007. DOI: 10.1016/B0-44-452747-8/00100-9
7. BARTON, C. M. The geology of South Shetland Islands. III, The stratigraphy of King George Island. British Antarctic Survey Report, v. 44, p. 1-33, 1965.
8. BAS. Geologic Map of Northen of Antarctic Peninsula. **British Antarctic Survey**, Folio 12, 1:1.000.000. 1969.
9. BENN, D.I.; HULTON, N.R.J. An Excel™ spreadsheet program for reconstructing the surface profile of former mountain glaciers and ice caps. **Remote Sensing**, v. 36, p. 605-610. 2010. DOI: 10.1016/j.cageo.2009.09.016
10. BENN, D.I.; COWTON, T.; TODD, J.; LUCKMAN, A. Glacier Calving in Greenland. **Current Climate Change Reports**, v. 3, p. 282–290, 2017. DOI: 10.1007/s40641-017-0070-1
11. BENN, D.I.; EVANS, D.J.A. **Glaciers and glaciation**. 2a ed. London: Hodder Education, 2010. 802p.
12. BENNETT M.R.; GLASSER, N.F. **Glacial geology – ice sheets and landforms**. England: John Wiley & Sons Ltd. 1996. 364 p.
13. BIANCHI, T.S.; ARNDT, S.; WILLIAN, E.N.A.; BENN, D.I.; BERTRAND, S.; CUI, X.; FAUST, J.; KOZIOROWSKA-MAKUCH, J.; CHRISTOPHER, M.M.; SAVAGE, C.; SMEATON, C.; SMITH, R.; SYVITSKI, J. Fjords as Aquatic Critical Zones (ACZs). **Earth Science Review**, v. 203, p. 103145, 2020. DOI: 10.1016/j.earscirev.2020.103145
14. BIRKENMAJER K. Tertiary glaciation in the South Shetland Islands, west Antarctica: evaluation of data. In: THOMSON, M.R.A.; CRAME, J.A.; THOMSON, J.W. (Ed.). **Geological evolution of Antarctica**. Cambridge: Cambridge University Press, 1991. p. 627-632.

15. BRADWELL, T.; SIGURÐSSON, O.; EVEREST, J. Recent, very rapid retreat of a temperate glacier in SE Iceland. **Boreas**, v. 42, p. 959–973. 2013. DOI: 10.1111/bor.12014
16. BRAUN, M.; SIMÕES, J.C.; VOGT, S.; BREMER, U.F.; BLINDOW, N.; PFENDER, M.; SAURER, H.; AQUINO, F.E.; FERRON, F.A. An improved topographic database for King George Island: compilation, application and outlook. **Antarctic Science**, v. 13, n.1, 2001. DOI:10.1017/s0954102001000074
17. BRAUN, M.; GOßMANN, H. Glacial Changes in the Areas of Admiralty Bay and Potter Cove, King George Island, Maritime Antarctica. In: BEYER, L.; BÖLTER, M. (Ed.). **Geoecology of Antarctic Ice-Free Coastal Landscapes**, Berlin, Heidelberg: Springer, 2002. p. 75 - 89.
18. CARRASCO, J.F.; BOZKURT, D.; CORDERO, R.R. A review of the observed air temperature in the Antarctic Peninsula. Did the warming trend come back after the early 21st hiatus?. **Polar Science**, v. 28, 100653, 2021. DOI: 10.1016/j.polar.2021.100653
19. CHANDLER, B.M.P.; LOVELL, H.; BOSTON, C.M.; LUKAS, S.; BARR, I.D.; BENEDIKTSSON, Í.Ö.; BENN, D.I.; CLARK, 502 C.D.; DARVILL, C.M.; EVANS, D.J.A.; EWERTOWSKI, M.W.; LOIBL, D.; MARGOLD, M.; OTTO, J.; ROBERTS, D.H.; 503 STOKES, C.R.; STORRAR, R.D.; STROEVEN, A.P. Glacial geomorphological mapping: A review of approaches and 504 frameworks for best practice. Earth-Science Reviews, 185, p. 806–846. 2018. DOI:10.1016/j.earscirev.2018.07.015
20. CONGEDO, L. Semi-Automatic Classification Plugin Documentation. Release 6.0.1.1. 2016. Disponível em: <DOI:10.13140/RG.2.2.29474.02242/1>. Acesso em: 18 de novembro de 2021.
21. CURL, J.E. **A glacial history of the South Shetland Islands, Antarctic**. Institute of Polar Studies Report, The Ohio State University, v. 63, 129 p. 1980.
22. DOWDESWELL, J.A.; Ó COFAIGH, C.; PUDSEY C.J. Thickness and extent of the subglacial till layer beneath an Antarctic paleo–ice stream. **Geology**, v. 32, p. 13–16, 2004. DOI: 10.1130/G19864.1
23. DOWDESWELL, J.A.; OTTESEN, D.; EVANS, J.; Ó COFAIGH, C.; ANDERSON J.B. Submarine glacial landforms and rates of ice-stream collapse. **Geology**, v. 36, n. 10, p. 819-822, 2008. DOI: 10.1130/G24808A.1
24. DZIEMBOWSKI, M.; BIALIK, R.J. The Remotely and Directly Obtained Results of Glaciological Studies on King George Island: A Review. Remote Sensing, v. 14, n. 12, p. 2736. 2022. DOI: 10.3390/rs14122736
25. Esri Inc. **ArcMap (versão 10.5.1)**. Redlands, Estados Unidos, 2016.
26. EVANS, D.J.A.; YOUNG, N.J.P.; Ó COFAIGH, C. Glacial geomorphology of terrestrial-terminating fast flow lobes/ice stream margins in the southwest Laurentide Ice Sheet. **Geomorphology**, 204, p. 86–113. 2014. DOI: 10.1016/j.geomorph.2013.07.031
27. FASTOOK, J.L.; HUGHES, T.J. New perspectives on paleoglaciology. **Quaternary Science Reviews**, v. 80, p. 169–194, 2013. DOI: 10.1016/j.quascirev.2013.08.023
28. FITZPATRICK, A.A.W.; HUBBARD, A.; JOUGHIN, I.; QUINCEY, D.J.; VAN AS, D.; MIKKELSEN, A.P.B.; DOYLE, S.H.; HASHOLT, B.; JONNES, G.A. Ice flow dynamics and surface meltwater flux at a land-terminating sector of the Greenland ice sheet. **Journal of Glaciology**, v. 59, n, 216, 2013. DOI:10.3189/2013JoG12J143
29. GERRISH, L.; FRETWELL, P.; COOPER, P. High resolution vector polylines of the Antarctic coastline (7.3) UK Polar Data Centre, Natural Environment Research Council, UK Research & Innovation. 2020. Disponível em: <https://www.add.scar.org/>. Acesso em: 18 de novembro de 2021.
30. GLASSER, N.F.; JANSSON, N.K.; HARRISON, S.; RIVERA, A. Geomorphological evidence for variations of the North Patagonian Icefield during the Holocene. **Geomorphology**, v. 71, p. 263–277. 2005. DOI: 10.1016/j.geomorph.2005.02.003
31. GLIMS. Global Land Ice Measurements from Space. Available in: http://www.glims.org/ Acess in:15/01/2021.
32. GRIBENSKI, N.; JANSSON, K.N.; LUKAS, S.; STROEVEN, A.P.; HARBOR, J.M.; BLOMDIN, R.; IVANOV, M.N.; HEYMAN, J.; PETRAKOV, D.A.; RUDOY, A.; CLIFTON, T.; LIFTON, N.A.; CAFFEE, M.W. Complex patterns of glacier

advances during the late glacial in the Chagan Uzun Valley, Russian Altai. **Quaternary Science Reviews**, v. 149, p. 288–305, 2016. DOI: 10.1016/j.quascirev.2016.07.032

33. HALL. B.L. Late-Holocene advance of the Collins ice cap, King George Island, South Shetland islands. **The Holocene**, v. 17, n. 8, p. 1253-1258, 2007. DOI: 10.1177/0959683607085132
34. HILL, E.; CARR, J.R.; STOKES, C.R.; GUDMUNDSSON, G.H.; Dynamic changes in outlet glaciers in northern Greenland from 1948 to 2015. **The Cryosphere**, v. 12, p. 3243–3263, 2018. DOI: 10.5194/tc-12-3243-2018
35. HILLEBRAND, F.L.; ROSA, C.N.; BREMER, U.F. Mapeamento das zonas de neve úmida e de percolação por meio do Sentinel-2. **Anuário do Instituto de Geociências**, v. 41, n. 3, p. 96–103, 2019. DOI:10.11137/2018_3_96_103
36. HUYBRECHTS, P.; DE WOLDE, J. The dynamic response of the Greenland and Antarctic Ice Sheets to multiple-century climatic warming. **Journal of Climate**, v. 12, p. 2169–2188. 1999. DOI: 10.1175/1520-0442(1999)012<2169:TDROTG>2.0.CO;2
37. KEJNA, M.; ARAZNY, A.; SOBOTA, I. Climatic change on King George Island in the years 1948 – 2011. **Polish Polar Research**, v. 34, n. 2, p. 213-235, 2013. DOI: 10.2478/popore−2013−0004
38. LI, C.; MICHEL, C.; SELAND GRAFF, L.; BETHKE, I.; ZAPPA, G.; BRACEGIRDLE, T.J.; FISCHER, E.; HARVEY, B.J.; IVERSEN, T.; KING, M.P.; KRISHNAN, H.; LIERHAMMER, L.; MITCHELL, D.; SCINOCCA, J.; SHIOGAMA, H.; STONE, D.; WETTSTEIN, J.J. Mid Latitude atmospheric circulation responses under 1.5 and 2.0 °C warming and implications for regional impacts. **Earth System Dynamics**, v. 9, p. 359–382, 2018. DOI: 10.5194/esd-9-359-2018
39. LI, Z., FANG, H., TIAN, L., DAI, Y., & ZONG, J.Changes in the glacier extent and surface elevation 370 in Xiongcaigangri region, Southern Karakoram Mountains, China. **Quaternary International**, 371, 371 67-75. 2015.
40. LI, D.; SHANGGUAN, D.; ANJUM, M.N. Glacial Lake inventory derived from Landsat 8 OLI in 2016–2018 in China–Pakistan economic corridor. **International Journal of Geo-Information**, v. 9, n. 5, 2020. DOI: 10.3390/ijgi9050294
41. LIANG, Q.; PENG, S.; NIU, B.; ZHOU, C.; WANG, Z. Mapping glacier-related research in polar regions: a bibliometric analysis of research output from 1987 to 2016. **Polar Research**, v. 37, 2018. DOI: 10.1080/17518369.2018.1468196.
42. LIVERMORE, R.A.; WOOLLETT, R.W. Seafloor spreading in the Weddell Sea and southwest Atlantic since the Late Cretaceous. **Earth and Planetary Science Letters**, v. 117, n. 3, p. 475–495, 1993. DOI: 10.1016/0012-821X(93)90098-T
43. LORENZ, J.L. **Variações de área das geleiras e o estado atual da linha de neve transitória dos campos de gelo da ilha Rei George, Antártica, usando sensores remotos orbitais**. Monografia (Bacharelado em Geografia). Universidade Federal do Rio Grande do Sul, Instituto de Geociências, Porto Alegre-RS. 2021.
44. MACKINTOSH, A.N.; ANDERSON, B.M.; PIERREHUMBERT, R.T. Reconstructing Climate from Glaciers. **Annual Review of Earth and Planetary Sciences**, v. 45, p. 649–680, 2016. DOI: 10.1146/annurev-earth-063016-020643
45. MALDONADO, A.; ZITELLINI, N.; LEITCHENKOV, G.; BALANYA, J.C.; COREN, F.; GALINDO-ZALDÍVAR, J.; LODOLO, E.; JABALOY, A.; ZANOLLA, C.; RODRÍGUEZ-FERNÁNDEZ, J.; VINNIKOVSKAYA, O. Small ocean basin development along the Scotia–Antarctica plate boundary and in the northern Weddell Sea. **Tectonophysics**, v. 296, n. 3, p. 371–402, 1998. DOI: 10.1016/S0040-1951(98)00153-X
46. MATSUOKA, K.; SKOGLUND, A.; ROTH G. 2018. Quantarctica [Dataset]. Norwegian Polar Institute.
47. MATSUOKA, K.; SKOGLUND, A.; ROTH, G.; DE POMEREU, J.; GRIFFITHS, H.; HEADLAND, R.; HERRIED, B.; KATSUMATA, K.; BROCQ A.; LICHT, K; MORGAN, F.; NEFF P.D.; RITZ, C.; SCHEINERT M.; TAMURA, T.; VAN DE PUTTE, A.; BROEKE, M.; DESCHWANDEM A.; DESCHAMPS-BERGER, C.; LIEFFERINGE, B.; TRONSTAD, S.; MELVÆR, Y. Quantarctica, an integrated mapping environment for Antarctica, the Southern Ocean, and sub-Antarctic islands. **Environmental Modelling & Software**, v.140, 105015, 2021. DOI: 10.1016/j.envsoft.2021.105015
48. MULVANEY, R.; ABRAM, N.J.; HINDMARSH, R.C.A. ARROWSMITH, C.; FLEET, L.; TRIEST, J.; SIME, L.C.; ALEMANY, O.; FOORD, S. Recent Antarctic Peninsula warming relative to Holocene climate and ice-shelf history. **Nature**, v. 489, n. 7414, p.141-144, 2012. DOI: 10.1038/nature11391.

49. NIE, Y.; LIU, Q.; LIU, S. Glacial Lake Expansion in the Central Himalayas by Landsat Images, 1990–2010. **PLOS ONE**, v. 9 p. e92654. 2013. DOI: 10.1371/journal.pone.0083973
50. OLIVA, M.; ANTONIADES, D.; SERRANO, E.; GIRALT, S.; LIU, E.J.; GRANADOS, I.; PLA-RABES, S.; TORO, M.; HONG, S.G.; VIEIRA, G. The deglaciation of Barton Peninsula (King George Island, South Shetland Islands, Antarctica) based on geomorphological evidence and lacustrine records. **Polar Record**, v. 55, n. 3, p. 177-188, 2019. DOI: 10.1017/S0032247419000469
51. OLIVA, M.; NAVARRO, F.; HRBÁCEK, F.; HERNÁNDEZ, A.; NÝVLT, D.; PEREIRA, P.; RUIZ-FERNÁNDEZ, J.; TRIGOD, R. Recent regional climate cooling on the Antarctic Peninsula and associated impacts on the cryosphere. Science of Total Environments, v. 580, p. 210–223, 2017. DOI: 10.1016/j.scitotenv.2016.12.030
52. OSMANOĞLU, B.; BRAUN, M.; HOCK, R.; NAVARRO, F. Surface velocity and ice discharge of the ice cap on King George Island, Antarctica. **Annals of Glaciology**, v. 54, n. 63, p.111–119, 2013. DOI: 10.3189/2013AoG63A517
53. OTTESEN, D.; DOWDESWELL, J.A. Assemblages of submarine landforms produced by tidewater glaciers in Svalbard**. Journal of Geophysical Research**, v. 111. 2006. DOI: 10.1029/2005JF000330
54. PERONDI, C.; ROSA, K.K.; VIEIRA, R. Caracterização geomorfológica das áreas livres de gelo na margem leste do campo de gelo Warszawa, ilha Rei George, Antártica Marítima. **Revista Brasileira de Geomorfologia**, v. 20, n. 2, 2019. DOI: 10.20502/rbg.v20i2.1433
55. PERONDI, C.; ROSA, K.K.; PETSCH, C.; IDALINO, F.D.; OLIVEIRA, M.A.G.; LORENZ, J.L.; VIEIRA, R.; SIMÕES, J.C. Recentes alterações nas geleiras e nos sistemas paraglaciais, Antártica Marítima. Revista **Geociências NE**, v. 6, 2020. DOI: 10.21680/2447-3359.2020v6n2ID19301
56. PERONDI, C.; ROSA, K.K.; VIEIRA, R.; MAGRANI, F.J.G.; AYRES-NETO, A.; SIMÕES. J. C. Geomorphology of Martel Inlet, King George Island, Antarctica: a new interpretation based on multi-resolution topo-bathymetric data. **Anais da Academia Brasileira de Ciências**, n. 94, p. 1-20. 2022. DOI: 10.1590/0001-3765202220210482
57. PETSCH, C.; ROSA, K.K.; VIEIRA, R.; BRAUN, M.H.; COSTA, R.M.; SIMÕES. J.C. The effects of climatic change on glacial, proglacial and paraglacial systems at Collins Glacier, King George Island, Antarctica, from the end of the Little Ice Age to the 21st century. **Investigaciones Geográficas**, n. 103, 2020. DOI: 10.14350/rig.60153
58. POPE, A. Antarctica Bedmap2 [Dataset]. University of Edinburgh. 2017. DOI: 10.7488/ds/1916.
59. POWELL, R.D.; ALLEY, R.B. Grounding-Line Systems: Processes, Glaciological Inferences and the Stratigraphic Record, in Geology and Seismic Stratigraphy of the Antarctic Margin. **Antarctic Research Series**, v. 2, p. 169-187, 2013. DOI: 10.1029/AR071p0169
60. PUDEŁKO, R.; ANGIEL, P.; POTOCKI, M.; JĘDREJEK, A.; KOZAK, M. Fluctuation of Glacial Retreat Rates in the Eastern Part of Warszawa Icefield, King George Island, Antarctica, 1979–2018. **Remote Sensing**, v. 10, n. 6, 2018. DOI:10.3390/rs10060892
61. RACHLEWICZ, G. Mid-winter thawing in the vicinity of Arctowski Station, King George Island. **Polish Polar Research**, v. 18, n. 1, p. 15 - 24. 1997. DOI:
62. RIGNOT, E.; STEFFEN, K. Channelized bottom melting and stability of floating ice shelves. Geophysical **Research Letters**, v. 35, p. 2–6, 2008. DOI: 10.1029/2007GL031765
63. ROSA, K.K.; PERONDI, C.; VEETTIL, B.K.; AUGER, J.D.; SIMÕES, J.C. Contrasting responses of land-terminating glaciers to recent climate variations in King George Island, Antarctica. Antarctic Science, v. 32, n. 5, p. 398–407, 2020. DOI: 10.1017/S0954102020000279
64. ROSA, K.K.; VIEIRA, R.; FERNADEZ, G.B.; SIMÕES, F.L.; SIMÕES, J.C. Glacial landforms and glaciological processes of the temperate Wanda glacier, South Shetlands**. Investigaciones Geográficas**, v. 43, p. 3 – 16, 2011.

65. ROSA, K.K.; VIEIRA, R.; MENDES, J.R.C.; SOUZA, J.R.; SIMÕES, J.C. Compilation of geomorphological map for reconstructing the deglaciation of ice-free areas in the Martel inlet, King George Island, Antarctic. Revista **Brasileira de Geomorfologia**, v. 14, p. 181-187, 2013. DOI: 10.20502/rbg.v14i2.324
66. ROSA, K.K.; MENDES, C.W.; VIEIRA, R.; DANI, N.; SIMÕES, J.C. Análise morfométrica do setor norte da Baía do Almirantado, Ilha Rei George, Shetlands do Sul, Antártica. **Boletim de Geografia**, v. 32, n. 1, p. 52-61, 2014a. DOI: 10.4025/bolgeogr.v32i1.18710
67. ROSA, K.K.; FREIBERGER, V.L.; VIEIRA, R.; ROSA, C.A; SIMÕES, J.C. Mudanças glaciais recentes e variabilidade climática na ilha Rei George, Antártica. **Quaternary and Environmental Geosciences Review**, v. 5, n. 2. 2014, p. 176 – 183, 2014b. DOI: 10.5380/abequa.v5i2.36642
68. RÜCKAMP, M.; BRAUN, M.; SUCKRO, S.; BLINDOW, N. Observed glacial changes on the King George Island ice cap, Antarctica, in the last decade. **Global and Planetary Change**. v. 79, p. 99–109, 2011. DOI: 10.1016/j.gloplacha.2011.06.009
69. SCHÄFER, M.; MÖLLER, M.; ZWINGER, T.; MOORE, J. Dynamic modeling of future glacier changes: mass-balance/elevation feedback in projections for the Vestfonna ice cap, Nordaustlandet, Svalbard**. Journal of Glaciology**, v. 61, p. 1121–1136. 2015. DOI: 10.3189/2015JoG14J184
70. SETZER, A.W.O.; FRANCELINO, M.R.; SCHAEFER, C.E.G.R.; COSTA, L.V.; BREMER, U.F. Regime climático na Baía do Almirantado: relações com o ecossistema terrestre. In: SCHAEFER, C. (Ed.). **Ecossistemas costeiros e monitoramento ambiental da Antártica Marítima**. Minas Gerais: Viçosa, 2004. p. 1–13.
71. SIEGERT, M.; ATKINSON, A.; BANWELL, A.; BRANDON, M.; COVEY, P.; DAVIES, B.; DOWNIE, R.; EDWARDS, T.; HUBBARD, B.; MARSHALL, G.; ROJELL, J.; RUMBLE, J.; STROEVE, J.; VAUGHAN, D. The Antarctic Peninsula Under a 1.5°C Global Warming Scenario. **Frontiers in Environmental Science**, v. 28, 2019. DOI: 10.3389/fenvs.2019.00102
72. SIEGERT, M.; FLORINDO. F.; DE SANTIS, L.; NAISH, T.R. The future evolution of Antarctic climate: conclusions and upcoming programmes. In: SIEGERT, M.; FLORINDO. F.; DE SANTIS, L.; NAISH, T.R. (Eds.). **Antarctic Climate Evolution**. Second Edition, Elsevier, p. 769-775. 2022. DOI: 10.1016/B978-0-12-819109-5.00005-0.
73. SIMÕES, J.C. Glossário da língua portuguesa da neve, do gelo e termos correlatos. **Pesquisa Antártica Brasileira**, p. 119 – 154, 2004.
74. SIMÕES, C.L. **Retração das geleiras Drummond e Widdowson em respostas às recentes mudanças ambientais na Península Antártica (1957 - 2016).** Dissertação (Mestrado em Geografia) - Instituto de Geociências, Universidade Federal do Rio Grande do Sul, Porto Alegre. 2017. 80 p.
75. SIMÕES, C.L.; ROSA, K.K.; CZAPELA, F.F.; VIEIRA, R.; SIMÕES, J.C. Collins glacier retreat process and regional climatic variations, King George Island, Antarctica. Geographical Review, v. 105, n. 4, p. 462 – 471, 2015. DOI: 10.1111/j.1931-0846.2015.12091.x
76. SMITH, J.; ANDERSEN, T.; SHORTT, M.; GAFFNEY, A.M.; TRUFFER, M.; STANTON, T.P.; BINDSCHADLER, R.; DUTRIEUX, P.; JENKINS, A.; HILLENBRAND, C.D.; EHRMANN, W.; CORR, H.F.J.; FARLEY, N.; CROWHURST, S.; VAUGHAN, D.G. Sub-ice-shelf sediments record history of twentieth-century retreat of Pine Island Glacier. **Nature**, v. 541, p. 77–80, 2017. DOI: 10.1038/nature20136.
77. STREUFF, K.; FORWICK, M.; SZCZUCINSKI, W. ANDREASSEN. K.; Ó COFAIGH, C. Submarine landform assemblages and sedimentary processes related to glacier surging in Kongsfjorden, Svalbard. **ArKtos**, v. 1, n. 14, 2015. DOI: 10.1016/j.margeo.2017.09.006
78. THOMAS, R.; FREDERICK, E.; KRABILL, W.; MANIZADE, S.; MARTIN, C. Recent changes on Greenland outlet glaciers. **Journal of Glaciology**, v. 55, p. 147–162, 2018. DOI: 10.3189/002214309788608958
79. TRUEBA, J.J.C.; CAÑADAS, E.S. El método AAR para la determinación de paleo-ELAs: análisis metodológico y aplicación en el macizo de Valdecebollas (Cordillera Cantábrica). **Cuadernos de Investigación Geográfica**, n. 30, p. 7-34, 2004. DOI: 10.18172/cig.1133

80. WÖLFL, A.C.; WITTENBERG, N.; FELDENS, P.; HASS, H.C.; BETZLER, C.; KUHN, G. Submarine landforms related to glacier retreat in a shallow Antarctic fjord. **Antarctic Science**, v. 28, p. 475–486, 2016. DOI: 10.1017/S0954102016000262
81. YOON, H.H.; PARK, B.K.; KIM, Y.; KIM, D. Glaciomarine sedimentation and its palaeoceanographic implications along the fiord margins in the South Shetland Islands, Antarctica during the last 6000 years. **Paleogeography, Palaeoclimatology, Paleoecology**, n. 157, p. 189-211, 2000. DOI: 10.1016/S0031-0182(99)00165-0